EXPERIMENTAL STUDY ON THE IMPACT OF ANCHOR LOSSES ON THE QUALITY FACTOR OF CONTOUR MODE ALN RESONATORS

J.Segovia-Fernandez[1], M.Cremonesi[2], C.Cassella[1], A.Frangi[2], and G.Piazza[1]
[1]Carnegie Mellon University, Pittsburgh, USA
[2]Politecnico of Milano, Italy

ABSTRACT

This paper presents an experimental study on the impact of anchor losses on the quality factor (Q) of laterally vibrating AlN contour mode resonators for three different resonance frequency devices (220 MHz, 370 MHz, and 1.05 GHz). Anchors of different width (W_a) and length (L_a) were designed as supports for resonators having a vibrating body of identical dimensions. The results confirm that the main source of damping is associated with anchor losses at 220 MHz and interfacial losses at 1.05 GHz. Furthermore, finite element analysis (FEA) was used to model anchor losses in AlN CMRs, exhibiting excellent agreement with the measurements.

KEYWORDS

AlN contour mode resonator, quality factor, anchor losses, interfacial losses, finite element analysis.

INTRODUCTION

The adoption of MEMS resonators for timing and frequency control applications as replacements for quartz crystals and surface acoustic wave (SAW) devices is highly dependent on the ability of this technology to achieve a high quality factor, Q, and electromechanical coupling, k_t^2, in a small form factor. AlN Contour Mode Resonators (CMR), a new class of piezoelectric MEMS transducers that can enable RF reconfigurable front-ends [1], have already shown reasonably high k_t^2, but limited Qs. Nevertheless, high Q is essential to reduce the phase noise in oscillators, and the insertion loss in filters. Therefore, there is a clear need of understanding the source of energy loss in AlN CMRs with the objective of improving the device design and, ultimately, increasing its Q. Although AlN CMRs have shown promising performance for RF applications, no comprehensive study of the loss mechanisms has ever been conducted for this type of MEMS devices.

Previous studies performed on MEMS resonators have suggested that in the high frequency range (200 MHz - 1 GHz) viscous damping can be excluded from the main sources of damping [2]. Additionally, it has been shown that AlN is an intrinsically high Q material [3, 4]. Therefore we hypothesize that damping in AlN CMRs can be primarily attributed to interfacial dissipation [5] and anchor losses [1]. The former arises from stress discontinuity at the interface between electrode and AlN layers. The latter depends on acoustic energy escaping the resonator through the anchors and being dissipated into the substrate. Anchor losses have been considered as the primary source of damping in traditional MEMS cantilever beams and analytical expressions to compute Q can be found in literature [6].

This work is mainly focused on experimentally verifying the impact of anchor geometry on the AlN CMR Q. For this purpose, three devices with different resonant frequencies (f_r) (220 MHz, 370 MHz, and 1.05 GHz) and various anchor sizes have been designed, fabricated, and tested (see Figure 1). For each frequency, the vibrating body dimensions were kept fixed, whereas the anchors' width (W_a) and length (L_a) were varied as a function of the wavelength (λ) associated with the fundamental mode of vibration of the resonator. To validate the experimental trend and develop a tool for predicting anchor losses and guide future resonator design, an ad-hoc finite element code to model anchor loss damping for AlN CMRs was also developed.

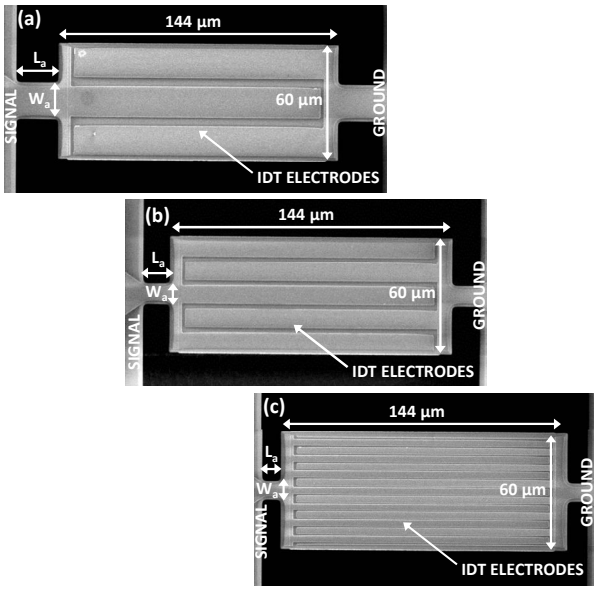

Figure 1: SEM of the (a) 220MHz, (b) 370MHz, and (c) 1.05GHz AlN CMRs.

DEVICE DESIGN AND FABRICATION

The principle of operation of AlN CMRs and the device description have been introduced in previous papers [1]. All the devices employed in this study are also known as one port Lateral Field Excited (LFE) resonators [1]. The resonators are formed by a vibrating AlN plate sandwiched between a bottom metal plate and a patterned top electrode. Interdigitated metal lines connected alternatively to signal and ground voltages form the top electrode. These electrodes generate the electric field lines across the piezoelectric material. The field lines are directed primarily along the thickness of the film by the presence of the bottom floating plate (Figure 2).

The resonance frequency (f_r) of these devices is set by two parameters: the electrode pitch (or finger width (W_f)) and the acoustic velocity of the resonator stack $(E/\rho)^{1/2}$. For this work, resonators with three different f_r (220, 370, and 1050 MHz) corresponding to three

different W_f (20, 12, and 4 µm) were designed and fabricated. All the devices were designed to have the same resonator body dimensions and electrode coverage (hence, distinct number of fingers). The width (W_r) and length (L_r) of the resonators were set to 60 and 144 µm, respectively. The metal coverage was set to be 75 % of the resonator body. On the contrary, both anchor's width (W_a) and length (L_a) were varied as a multiple of the wavelength of the CMR (λ) (λ is equal to $2W_f$). Thus, devices with W_a/λ=1/4, 1/2, 1, and 3/2, and L_a/λ=1/4, 1/2, and 1 were designed for all the frequencies under study.

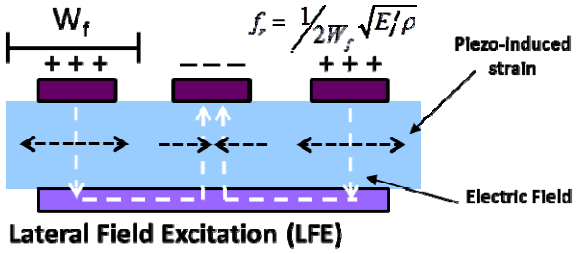

Figure 2: Cross section of a LFE AlN CMR and resonance frequency equation.

A three masks process is required to fabricate these devices (Figure 3). The AlN thickness is set to be 1 µm, and both electrode and bottom layers are selected to be around 100 nm, as previous demonstrations have shown to yield high Q devices with similar dimensions. The metals selected here are Pt for the bottom plate (this provides a good orientation for the AlN films) and Al for the top electrode (this reduces the top electrode resistance). Figure 4 shows an SEM image of a device cross section in which the angle of the AlN sidewall is shown to be 28.5°. As will be shown in the following section by finite element analysis (FEA), this angle is extremely important in setting the anchor losses in AlN CMRs.

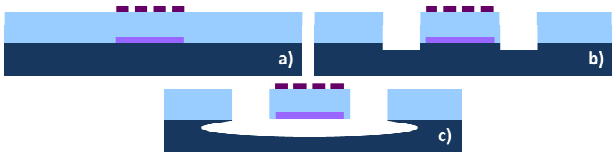

Figure 3: Schematic representation of the 3 mask fabrication process used for the making of LFE resonators: a) sputtering and patterning of the Pt bottom plate, sputtering of the AlN piezoelectric film, and sputtering and patterning of the Al top electrode; b) dry etching of AlN in Cl_2-based chemistry; and c) release of the AlN resonator in XeF_2 chemistry.

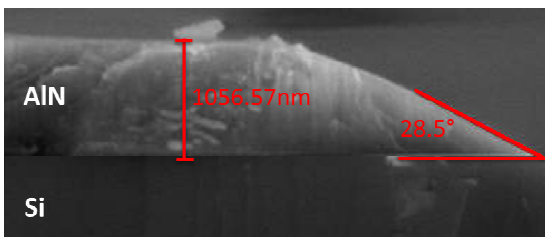

Figure 4: SEM of the cross section of the AlN sidewall. The sidewall is the result of a specific dry etching recipe using a patterned, post-baked photoresist as a hard mask.

EXPERIMENTAL TESTING AND DATA ANALYSIS

Experimental data were collected over a total of 432 AlN CMRs (144 for each f_r). For a fixed f_r, variations in W_a and L_a were tested for a total of 16 different combinations. These configurations were tested on 3 different chips belonging to the same wafer. Effectively, 9 repetitions (3 for each chip) were tested for each layout to ensure a minimum level of statistics for each device. To extract the electrical response (admittance) of the resonators an Agilent N5230A network analyzer was used. The values of the device quality factor (Q) were directly calculated as the ratio $f_r/\Delta f_{-3dBs}$ (for our study we neglect the impact of the electrical resistance on Q). Table 1 reports the average and standard deviation of the Qs recorded for 9 identical devices. Values are compared among the same frequency resonators having different W_a/λ, and L_a/λ. The highest and lowest Qs reported at a fixed L_a/λ are alternatively highlighted in green and red. On the other hand, no special trend is observed for a fixed W_a/λ.

Table 1: Average and standard deviation of the measured Q for a sample of 9 equivalent resonators at 220 MHz, 370 MHz, and 1.05 GHz.

		Quality factor					
		fs=220MHz		fs=370MHz		fs=1.05GHz	
Wa/λ	La/λ	Avg	Stand Dev	Avg	Stand Dev	Avg	Stand Dev
1/4	1/4	1532	448	1424	500		
1/2	1/4	2343	1014	1468	694	1331	510
1	1/4	520	150	667	267	1586	357
3/2	1/4	932	212	1116	386	1606	530
1/4	1/2	1356	414	1112	480		
1/2	1/2	2180	1184	1350	570	1183	460
1	1/2	718	249	841	302	1219	668
3/2	1/2	1201	336	1124	460	1634	453
1/4	1	1191	322	1183	392		
1/2	1	2318	938	1387	507	1189	465
1	1	773	206	1055	300	1496	491
3/2	1	1325	244	1132	408	1657	418

From the summarized data (Table 1) a clear trend relating the measured Q with W_a/λ is observed for both 220 and 370 MHz devices. Experimental results show that Q improves drastically when W_a/λ=1/2 and, on the contrary, a notable reduction of Q occurs when W_a/λ=1. On the other hand, no conclusions can be reached for 1.05 GHz resonators since only small variations in Q are observed. Figure 5 shows that as f_r increases the variations among the values of Q recorded for different anchor size resonators decreases. This fact indicates that at high frequencies the dominant source of losses in AlN CMRs is no longer anchor losses. At those frequencies interfacial dissipation starts to play a more significant role in the determination of Q. This is in line with what have been previously reported in the literature [7].

Considering only two major damping mechanisms, we can simplify the equation that determines the Q in AlN CMRs in the range of 200 MHz – 1 GHz as:

$$\frac{1}{Q}=\frac{1}{Q_{\text{int}}}+\frac{1}{Q_{anc}} \quad (1)$$

where $1/Q_{int}$ represents the damping due to interfacial dissipation and $1/Q_{anc}$ represents the losses due to the anchors.

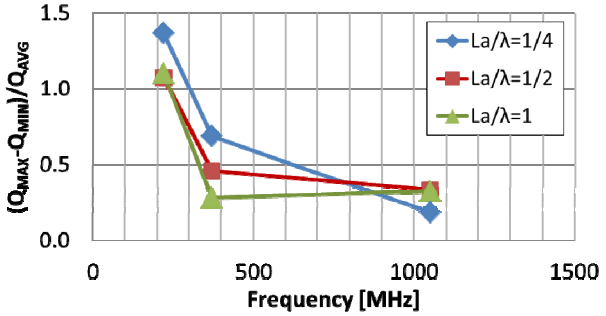

Figure 5: Relative variation of the measured Qs (Q_{MAX} and Q_{MIN} being respectively the maximum and minimum Q for a given device frequency) versus f_r at a fixed L_a/λ.

By assuming that the Q at 1 GHz is almost exclusively dominated by interfacial dissipation (Q_{int}), we can use this value as a reference to gauge the contribution of interfacial losses at lower frequencies. Since a slight dispersion of Q is observed at 1.05 GHz (Figure 5) we consider that this can be attributed to process variations (see standard deviation reported in Table 1) and we take the average value as a reference for Q_{int} at 1.05 GHz. Assuming a direct proportionality for Q_{int} with respect to frequency [7], the Q_{int} for both 370 and 220 MHz devices can be predicted. Note that simple proportional scaling can be performed as we have produced devices with the same exact metal coverage at all frequencies and the AlN plates all have the same size. Finally, the contribution to the device Q due to anchor losses (Q_{anc}) can be extracted by using Eq. (1) (Table 2). These values will be later used for comparison with the FEA simulations.

Table 2: Summary of the estimated Qs due exclusively to anchor losses (highlighted in yellow) assuming constant interfacial losses. Interfacial losses are considered the only source of damping at 1.05 GHz and their contribution is scaled with frequency for the devices vibrating at 370, and 220 MHz.

		f_0=1GHz	f_0=370MHz		f_0=220MHz		$\lvert Q_{anc}^{1}-Q_{anc}^{2}\rvert$
Wa/λ	La/λ	Q_{int}	Q_{int}	Q_{anc}^{1}	Q_{int}	Q_{anc}^{2}	
1/4	1/4	1433	4067	2192	6839	1974	217
1/2	1/4	1433	4067	2298	6839	3564	1266
1	1/4	1433	4067	797	6839	563	234
3/2	1/4	1433	4067	1537	6839	1079	458
1/4	1/2	1433	4067	1531	6839	1691	161
1/2	1/2	1433	4067	2020	6839	3200	1180
1	1/2	1433	4067	1060	6839	802	258
3/2	1/2	1433	4067	1553	6839	1456	97
1/4	1	1433	4067	1667	6839	1442	226
1/2	1	1433	4067	2105	6839	3506	1401
1	1	1433	4067	1424	6839	872	552
3/2	1	1433	4067	1569	6839	1643	74

ANALYSIS OF EXPERIMENTAL DATA BY THE FINITE ELEMENT METHOD

In order to predict anchor losses, it is generally accepted that all the elastic waves radiating from the anchors of the resonator into the elastic subspace are finally dissipated. From the numerical point of view this can be simulated using suitable absorbing conditions. Among the different options, the Perfectly Matched Layer (PML) technique has been adopted and a PML algorithm has been included in a dedicated large scale 3D numerical code. The approach has been described in details in [7, 8] where extensive validation for MEMS applications has been discussed. The same tool, suitably modified, is here applied to the analysis of the CMRs described in the previous sections.

Figure 6 shows the geometrical model of the devices employed in the numerical simulations where, exploiting the symmetry of the problem, only a quarter portion of the resonator has been discretized. All the geometrical features, including the proper sidewall angle are accurately reproduced, since this proves to be crucial for a correct prediction of the dissipation mechanisms.

In Figure 6 the level of refinement of the mesh employed in the simulation can be also appreciated (~170000 quadratic tetrahedra).

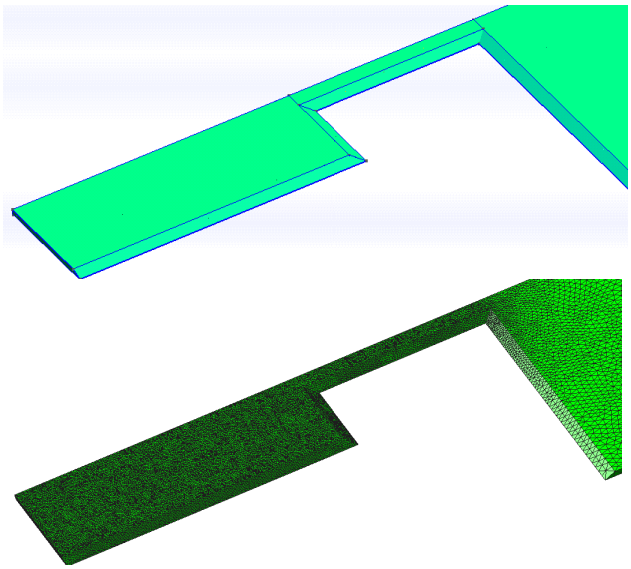

Figure 6: Geometry of a quarter portion of the fabricated and tested AlN CMR and mesh employed in the simulations.

Results of the numerical analyses are collected and presented on Figures 7 and 8. Thus, figure 7 shows a plot of the activated modes for a 220 MHz AlN CMR corresponding to the four experimental cases associated with different values of W_a/λ and a fixed value of L_a/λ=1. Then, figure 8 shows the simulated Q due to anchor losses as a function of W_a and at a fixed value of L_a/λ=1. The continuous line represents the numerical estimate and the circles denote the experimental data. As we can observe an excellent agreement among simulations and experimental results is found. The strong peak numerically predicted for widths slightly smaller than 20 µm is currently under verification with further experiments.

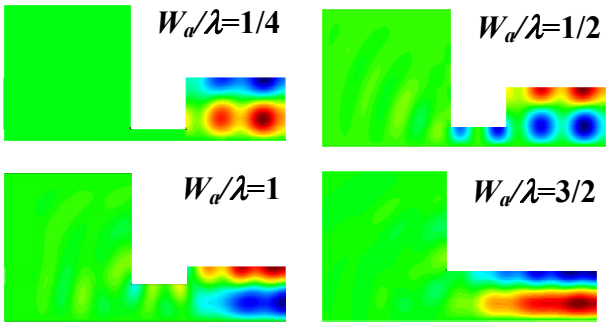

Figure 7: Results of the 3D FEM simulations of a 220 MHz AlN CMR (=40 μm). Parallel-to-the-plate displacement component simulated on a quarter portion of the whole resonator. For all the cases L_a=40 μm.

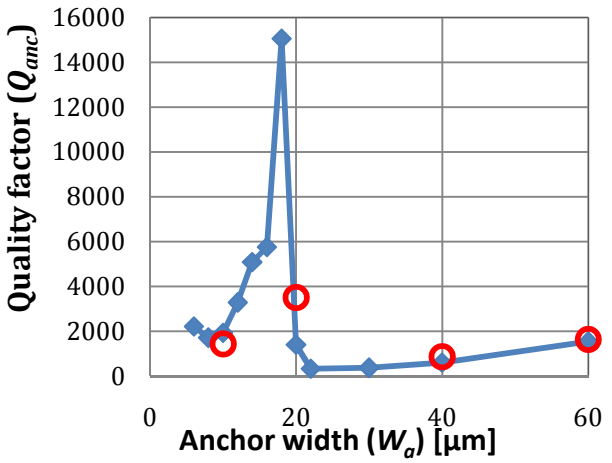

Figure 8: 3D FEM simulations of a 220MHz AlN CMR (=40 μm). Evolution of Q_{anc} at a varying W_a (L_a=40 μm); experimental results for the same geometry are overlapped as red circles.

The numerical model is then used as a predictive tool to simulate the sensitivity of the devices to the value of the sidewall angle. Figure 9 shows a plot of the quality factor due to anchor losses as a function of the angle. Indeed a strong dependence of ***Q*** on the AlN sidewall angle can be observed.

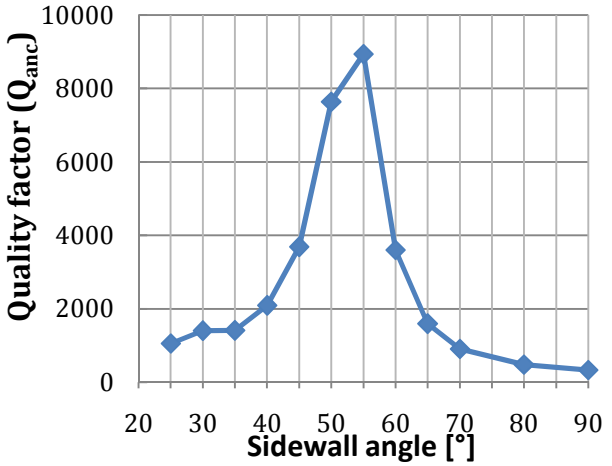

Figure 9: Results of 3D FEM simulations of a 220MHz AlN CMR (=40 μm). Evolution of Q_{anc} varying the sidewall angle (W_a=20μm).

CONCLUSIONS

The reported experimental results demonstrate that there exist a relationship between the anchor size and the *Q* of AlN CMRs working at 220 and 370MHz. According to the experiments the device *Q* exhibits a maximum when $W_a/\lambda=1/2$, and a minimum when $W_a/\lambda=1$. This is also confirmed by finite element analysis, which was introduced for the first time to model how anchor losses impact the *Q* of AlN CMRs. On the other hand, the experiments also confirmed that at higher operating frequencies (1 GHz) anchor losses are less dominant and interfacial losses play a more important role in determining the device *Q*.

ACKNOWLEDGEMENTS

The authors would like to thank the DEFYS DARPA contract # FA86501217624 for funding.

REFERENCES

[1] G. Piazza, P. J. Stephanou, A. P. Pisano, "Piezoelectric Aluminum Nitride Vibrating Contour-Mode MEMS Resonators", *Journal of MEMS*, vol. 15, no. 6, pp. 1406-1418, 2006.

[2] R. Lifshitz, M.L. Roukes, "Thermoelastic damping in micro- and nanomechanical systems", *Phys. Rev. B*, vol. 61, pp. 5600–5609, 2000.

[3] S. Gong, N.-K. Kuo, and G. Piazza, "GHz high Q lateral overmoded bulk acoustic wave resonators with fxQ of 1.17x10e13," in *Proc. of IFCS*, pp. 1-5, 2011.

[4] L.-W. Hung and C. T.-C. Nguyen, "Capacitive piezo transducers for higher Q contour-mode AlN resonators at 1.2 GHz," *Solid-State Sensor and Actuator Workshop*, pp. 463-466, 2010.

[5] J. Segovia-Fernandez, N- K. Kuo, G. Piazza, "Impact of metal electrodes on the figure of merit (kt2·Q) and spurious modes of contour mode AlN resonators", in *IUS 2012*, to be published.

[6] J. A. Judge, D. M. Photiadis, J. F. Vignola, B. H. Houston, J. Jarzynski, "Attachment losses of micromechanical and nanomechanical resonators in the limits of thick and thin support structures", *Journal of Applied Physics*, 2007.

[7] A. Frangi, M. Cremonesi, A. Jaakkola, T. Pensala, "Analysis of anchor and interface losses in piezoelectric MEMS resonators", *Sensors & Actuators: A Physical*, vol. 190, pp. 137-134, 2013.

[8] A. Frangi, A. Bugada, M. Martelo, P.T. Savadkoohi "Validation of PML-based models for the evaluation of anchor dissipation in MEMS resonators", *European Journal of Mechanics - A/Solids,* vol. 37, pp. 256-265, 2013

CONTACT

*J.Segovia-Fernandez; jsegovia@andrew.cmu.edu

*A.Frangi; attilio.frangi@polimi.it